Plasma-induced nonlinear optical phenomena in gas-filled hollow-core PCFs

Fabio Biancalana, and Mohammed F. Saleh

Citation: AIP Conference Proceedings **1475**, 6 (2012);

View online: https://doi.org/10.1063/1.4750077

View Table of Contents: http://aip.scitation.org/toc/apc/1475/1

Published by the American Institute of Physics

Plasma-induced nonlinear optical phenomena in gas-filled hollow-core PCFs

Fabio Biancalana and Mohammed F. Saleh

Max Planck Institute for the Science of Light, Günther-Scharowsky str. 1, 91058 Erlangen, Germany

Abstract. By using a new theoretical framework based on equations for the electric field envelope, we provide a complete theoretical explanation of several plasma-induced nonlinear optical phenomena, including the soliton self-frequency blueshift, recently observed experimentally in a gas-filled hollow-core PCF.

Keywords: Solitons, plasma physics, photonic crystal fibers, modulational instability, supercontinuum
PACS: 42.65.Re, 42.81.Dp, 42.65.Ky

Hollow-core photonic crystal fibre (HC-PCF) [1] with a kagomé-lattice cladding has recently been shown to be optimal for the investigation of broadband light-matter interactions between intense optical pulses and gaseous media. These fibers typically show transmission bands covering the visible and near-IR parts of the spectrum with relatively low loss and low group velocity dispersion (GVD), absence of surface modes, and high confinement of light in the core. Filled with a noble gas, they have recently been used in high-harmonic [2] and efficient deep UV generation from fs pump pulses at 800 nm [3]. It has been previously shown that the Raman threshold can be drastically reduced in a HC-PCF filled with a Raman-active gas (such as H_2) [4]. The system can be used for detailed experimental studies of, e.g., self-similar solutions of the sine-Gordon equation [5] and backward stimulated Raman scattering [6, 4]. The concept of soliton self-frequency blue-shift was introduced and predicted in [7]. A soliton blue-shift has been recently observed in tapered solid-core photonic crystal fibers where the zero-dispersion wavelength varies along the fiber [8]. In conventional bandgap-guiding gas-filled HC-PCFs, which have narrow bands of transmission, a limited ionization-induced blue-shift of guided ultrashort pulses has been reported [9]. In a recent groundbreaking experiment, ultrafast nonlinear dynamics in the ionization regime has been studied experimentally in Ar-filled kagomé-style HC-PCF [10]. The reasons for the success of kagomé HC-PCF in these applications are: (i) a group velocity dispersion (GVD) that is remarkably small [$|\beta_2| < 10$ fs^2/cm $\equiv 1$ ps^2/km from 400 to 1000 nm, see Fig. 1(a)] in comparison to solid-core fibers; (ii) the gas and waveguide contributions to the GVD can be balanced by varying the pressure, unlike in large-bore capillary-based systems where the normal dispersion of the gas dominates over the waveguide dispersion, see also Fig. 1(a). Photoionization in gases is traditionally modeled by using the full electric field of the pulse [11]. In this work, based on Ref. [12], we have first developed a new model to study pulse propagation in gas-filled HC-PCFs in terms of the complex *envelope* of the pulse. By using this model, we show analytically for the first time that intra-pulse photoionization leads to a soliton self-frequency blue-shift.

Photoionization can take place by either tunneling or multiphoton processes. These regimes are characterized by the Keldysh parameter p_K [11]. In the tunneling regime ($p_K \ll 1$) the time-averaged ionization rate $\mathscr{W}(I)$ is given by [13]

$$\mathscr{W}(I) = d\,(I_H/I)^{1/4}\,\exp[-b\,(I_H/I)^{1/2}], \qquad (1)$$

where $d \equiv 4\,\delta_0\,[3/\pi]^{1/2}\,[U_I/U_H]^{7/4}$, $b \equiv 2/3\,[U_I/U_H]^{3/2}$, $\delta_0 = 4.1\times10^{16}$ Hz is the characteristic atomic frequency, U_I is the ionization energy of the gas (~ 15.76 eV for argon), $U_H \approx 13.6$ eV is the ionization energy of hydrogen, $I_H = 3.6\times10^{16}$ W/cm^2 and I is the laser pulse intensity. For values of I in the range of 100 TW/cm^2, the Keldysh parameter is $p_K \lessapprox 1$ for noble gases. However, experiments show that tunneling models provide excellent agreement with the experimental measurements even for $p_K \approx 1$. As shown in Fig. 1(b), Eq. (1) predicts an ionization rate that is exponential-like for pulse intensities above a threshold value. Loss due to absorption of photons in the plasma is *proportional* to the ionization rate. Hence, any pulse with $I \gg I_{\rm th}$ will have its intensity strongly driven back to near the threshold value, resulting in a drastically reduced ionization loss. This allows us to use the first-order Taylor series to *linearize* the tunneling model just above $I = I_{\rm th}$, where the optical pulses can survive for relatively long time without appreciable attenuation. Expanding Eq. (1) in its linear regime around an arbitrary point $a = I_a/I_H$, results in $\mathscr{W} \approx \tilde{\sigma}\,\Delta I\,\Theta(\Delta I)$, where $\Delta I \equiv I - I_{\rm th}$, $\tilde{\sigma} = d\,e^{-x}\,(2x-1)/[4\,a^{5/4}\,I_H]$, $I_{\rm th} = a I_H (2x-5)/(2x-1)$ is the threshold intensity, $x = b/\sqrt{a}$, and a is chosen to reproduce

The Fifth International Workshop on Theoretical and Computational Nano-Photonics
AIP Conf. Proc. 1475, 6-8 (2012); doi: 10.1063/1.4750077

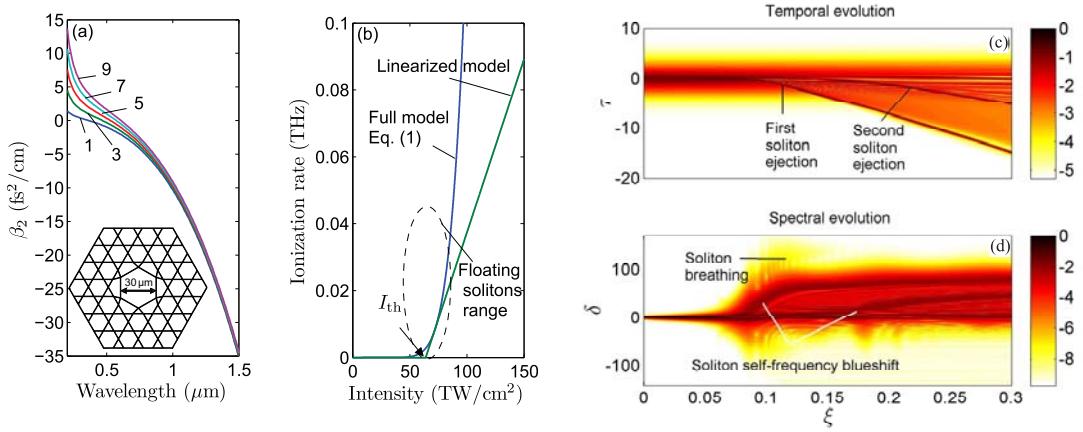

FIGURE 1. (a) GVD of an Ar-filled HC-PCF for gas pressures between 1 and 9 bar. All subsequent calculations in this work assume 5 bar pressure. Inset: cross-section of a broadband-guiding HC-PCF with a kagomé-lattice cladding and a core diameter 30 μm. Typical experimental transmission losses for the fundamental mode are 1 dB/m for at 800 nm. (b) Comparison of the dependence of the Ar ionization rate on the pulse intensity using the full model of Eq. (1) and the linearized model. (c,d) Respectively temporal and spectral evolution of an energetic pulse propagating in the Ar-filled HC-PCF. The temporal profile of the input pulse is $N\,\mathrm{sech}\,\tau$, with $N = 8$. The panels show the ejection of two fundamental solitons that continuously blue-shift until ionization loss reduces their intensities below the threshold value. Contour plots in this work are given in a logarithmic scale.

the physically observed threshold intensity in the fiber of Fig. 1(a), $a \cong 2\times10^{-3}$. The purpose of the Heaviside function Θ is to set the ionization rate to zero below the threshold intensity. As shown in Fig. 1(b), the linearized model underestimates the ionization rate and thus the ionization loss, in comparison to the full model. This leads to a similar qualitative behavior between the two models even for $I > I_{\rm th}$, since the ionization rate and the ionization loss are the key factors in the photoionization process.

One can prove from first principles that propagation of light in a HC-PCF filled with an ionized Raman-active gas can be then described by the following coupled equations [12]:

$$\begin{aligned}&\left[i\partial_z + \hat{D}(i\partial_t) + \gamma_{\rm K} R(t)\otimes|\Psi(t)|^2 - \frac{\omega_{\rm p}^2}{2k_0c^2} + i\alpha\right]\Psi = 0\\ &\partial_t n_{\rm e} = \left[\tilde{\sigma}/A_{\rm eff}\right]\left[n_{\rm T}-n_{\rm e}\right]\Delta|\Psi|^2\,\Theta\left(\Delta|\Psi|^2\right)\end{aligned}\quad , \tag{2}$$

where $\Psi(z,t)$ is the electric field *envelope*, z is the longitudinal coordinate along the fiber, t is the time in a reference frame moving with the pulse group velocity, $\hat{D}(i\partial_t) \equiv \sum_{m\geq2}\beta_m(i\partial_t)^m/m!$ is the full dispersion operator, β_m is the m-th order dispersion coefficient calculated at an arbitrary reference frequency ω_0, $\gamma_{\rm K}$ is the Kerr nonlinear coefficient of the gas, $R(t) = (1-\rho)\delta(t) + \rho\, h(t)$ is the normalized Kerr and Raman response function of the gas, $\delta(t)$ is the Dirac delta function, ρ is the relative strength of the non-instantaneous Raman nonlinearity, $h(t)$ is the causal Raman response function of the gas, the symbol $\otimes$ denotes the time convolution, c is the speed of light, $k_0 = \omega_0/c$, ω_0 is the pulse central frequency, $\omega_{\rm p} = [e^2 n_{\rm e}/(\varepsilon_0 m_{\rm e})]^{1/2}$ is the plasma frequency associated with an electron density $n_{\rm e}(t)$, e and $m_{\rm e}$ are the electron charge and mass, and ε_0 is the vacuum permittivity, $\alpha = \alpha_{\rm l} + \alpha_2$ is the total loss coefficient, $\alpha_{\rm l}$ is the fiber loss, $\alpha_2 = (A_{\rm eff}U_I)/(2|\Psi|^2)\,\partial_t n_{\rm e}$ is the ionization-induced loss term, $A_{\rm eff}$ is the effective mode area, $\Delta|\Psi|^2 = |\Psi|^2 - |\Psi|^2_{\rm th}$, $|\Psi|^2 = IA_{\rm eff}$, $|\Psi|^2_{\rm th} = I_{\rm th}A_{\rm eff}$, and $n_{\rm T}$ is the total number density of ionizable atoms in the fiber, associated with the maximum plasma frequency $\omega_{\rm T} \equiv [e^2 n_{\rm T}/(\varepsilon_0 m_{\rm e})]^{1/2}$. In these coupled equations, the recombination process is neglected since the pulse duration (of the order of tens of fs) is always shorter than the recombination time. If $|\Psi|^2$ is measured in W, $\tilde{\sigma}/cA_{\rm eff} \equiv \gamma_{\rm I}$ has the dimensions of $\mathrm{W}^{-1}\mathrm{m}^{-1}$. This is the nonlinearity associated with plasma formation in the fiber. According to recent experimental measurements, $\gamma_{\rm K}$ depends linearly on the gas pressure. These coupled equations (2) are the most important contribution of the present work.

In order to extract useful analytical information from Eqs. (2), further simplifications are necessary. For pulses with maximum intensities just above the ionization threshold (which we dub *floating* pulses), the ionization loss is not large and can be neglected to a first approximation. For such pulses, only a small portion of energy above the threshold intensity contributes to the creation of free electrons. Furthermore, for floating pulses one can remove the Θ-function from the equations, provided that the cross-section $\tilde{\sigma}$ is replaced by a properly reduced $\tilde{\sigma}'$ that takes into account the overestimation of

the ionization rate. Introducing the following rescalings and redefinitions: $\xi \equiv z/z_0$, $\tau \equiv t/t_0$, $\Psi_0 \equiv [\gamma_K z_0]^{-1/2}$, $\psi \equiv \Psi/\Psi_0$, $r(\tau) \equiv R(t)t_0$, $\phi \equiv \frac{1}{2}k_0 z_0 [\omega_p/\omega_0]^2$, $\phi_T \equiv \frac{1}{2}k_0 z_0 [\omega_T/\omega_0]^2$, and $\sigma \equiv \tilde{\sigma}' t_0/[A_{eff}\gamma_K z_0]$, where $z_0 \equiv t_0^2/|\beta_2(\omega_0)|$ is the second-order dispersion length at the reference frequency ω_0, and t_0 is the input pulse duration. Hence, the two coupled equations for floating pulses can be replaced by

$$\begin{array}{l} \left[i\partial_\xi + \hat{D}(i\partial_\tau) + r(\tau) \otimes |\psi(\tau)|^2 - \phi\right] \psi = 0 \\ \partial_\tau \phi = \sigma(\phi_T - \phi)|\psi|^2 \end{array} . \qquad (3)$$

The effect of the Raman and ionization perturbations on the soliton dynamics in HC-PCFs can be studied using Eqs. (3). The second equation can be solved analytically, $\phi(\tau) = \phi_T \left\{1 - e^{-\sigma \int_{-\infty}^{\tau} |\psi(\tau')|^2 d\tau'}\right\}$, with the initial condition $\phi(-\infty) = 0$, corresponding to the absence of any plasma before the pulse arrives. For a small ionization cross-section, $\phi(\tau) \simeq \eta \int_{-\infty}^{\tau} |\psi(\tau')|^2 d\tau'$, where $\eta \equiv \sigma\phi_T$. Moreover, in the long-pulse limit $|\psi(\tau - \tau')|^2 \simeq |\psi(\tau)|^2 - \tau' \partial_\tau |\psi(\tau)|^2$. This allows the two coupled equations to be reduced to a single partial integro-differential equation:

$$i\partial_\xi \psi + \hat{D}(i\partial_\tau)\psi + |\psi|^2\psi - \tau_R \psi \partial_\tau |\psi|^2 - \eta\psi \int_{-\infty}^{\tau} |\psi|^2 d\tau' = 0 \qquad (4)$$

where $\tau_R \equiv \int_0^\infty \tau' r(\tau')\, d\tau'$. This equation shows clearly that the effect of ionization is exactly opposite to that of the Raman effect: the fourth term in Eq. (4) involves a *derivative* of the field intensity, while the fifth term involves an *integral* of the same quantity. One can then conjecture that the last term will lead to a soliton self-frequency blue-shift due to ionization, instead of a red-shift due to Raman self-scattering [14]. This clearly shows that, in the range of validity of perturbation theory (i.e., for floating solitons), *photoionization leads to a soliton self-frequency blue-shift* [12]. This blue-shift is accompanied by a constant acceleration of the pulse in the time domain – opposite to the Raman effect, which produces pulse deceleration [14]. This blue-shift (distinct from the effects discussed in Ref. [7]) is limited only by ionization loss, which slowly decreases the pulse intensity until it falls below the threshold value.

In the presence of ionization-induced losses above the threshold intensity, Eqs. (2) must be numerically solved to study the full dynamics of floating pulses. Figures 1(c,d) show the temporal and spectral evolution of a high-order input soliton, closely following the results reported in [10]. When the intensity of the energetic pulse exceeds the threshold value as a result of self-compression, a fundamental soliton is ejected from the main pulse and continues to blue-shift until ionization loss reduces its amplitude below the threshold value. At longer distances, another compression occurs and a second soliton is generated. The use of a kagomé-style HC-PCF is essential to observe the soliton blue-shift, since conventional photonic-bandgap fibers have much stronger dispersion variations, which would quickly destabilize any possible solitary wave as in [9].

In conclusion, a direct photoionization process can act on solitons by constantly blue-shifting their central frequencies when the intensity of solitons is slightly above the photoionization threshold, thus representing the exact counterpart of the Raman self-frequency red-shift. This spectral transformation is limited only by the ionization losses. The new theoretical model, presented by Eqs. (2), is suitable for analytical calculations, and has led us to predict a number of other new phenomena such as long-range non-local correlation forces, and spectral transformation between red- and blue-shift in Raman-active gases, which we shall present at the conference. Our results reveal new physics and offer novel opportunities for the manipulation and control of the soliton dynamics inside these versatile optical waveguides.

REFERENCES

1. P. St.J. Russell, Science **299**, 358 (2003).
2. O. H. Heckl, C. R. E. Baer, C. Kränkel, S. V. Marchese, F. Schapper, M. Holler, T. Südmeyer, J. S. Robinson, J. W. G. Tisch, F. Couny, P. Light, F. Benabid, and U. Keller, Appl. Phys. B **97**, 369 (2009).
3. N. Y. Joly, J. Nold, W. Chang, P. Hölzer, A. Nazarkin, G. K. L. Wong, F. Biancalana, and P. St.J. Russell, Phys. Rev. Lett. **106**, 203901 (2011).
4. F. Benabid, J. C. Knight, G. Antonopoulos, and P. St.J. Russell, Science **298**, 399 (2002).
5. A. Nazarkin, A. Abdolvand, A. V. Chugreev and P. St.J. Russell, Phys. Rev. Lett. **105**, 173902 (2010).
6. A. Abdolvand, A. Nazarkin, A. V. Chugreev, C. F. Kaminski, and P. St.J. Russell, Phys. Rev. Lett. **103**, 183902 (2009).
7. V. N. Serkin and V. A. Vysloukh, in Nonlinear guided wave phenomena, Technical Digest, TUB **14**, pp. 236 (1993).
8. S. P. Stark, A. Podlipensky, and P. St.J. Russell, Phys. Rev. Lett. **106**, 083903 (2011).
9. A. B. Fedotov, E. E. Serebryannikov, and A. M. Zheltikov, Phys. Rev. A **76**, 053811 (2007).
10. P. Hölzer, W. Chang, J. C. Travers, A. Nazarkin, J. Nold, N. Y. Joly, M. F. Saleh, F. Biancalana, and P. St.J. Russell, Phys. Rev. Lett. **107**, 203901 (2011).
11. M. Geissler, G. Tempea, A. Scrinzi, M. Schnürer, F. Krausz, and T. Brabec, Phys. Rev. Lett. **83**, 2930 (1999).
12. M. F. Saleh, W. Chang, P. Hölzer, A. Nazarkin, J. C. Travers, N. Y. Joly, P. St. J. Russell and F. Biancalana, Phys. Rev. Lett. **107**, 203902 (2011)
13. P. Sprangle, J. R. Penano, and B. Hafizi, Phys. Rev. E **66**, 046418 (2002).
14. F. M. Mitschke and L. F. Mollenauer, Opt. Lett. **11**, 659 (1986).